

# Lowest Energy States of Small Pd Clusters Using Density Functional Theory and Standard ab Initio Methods. A Route to Understanding Metallic Nanoprobes

Angelica G. Zacarias,<sup>†</sup> Miguel Castro,<sup>‡</sup> James M. Tour,<sup>\*,§</sup> and Jorge M. Seminario<sup>\*,†</sup>

Department of Chemistry and Biochemistry, University of South Carolina, Columbia, South Carolina 29208; Departamento de Física y Química Teórica, Facultad de Química, Universidad Nacional Autónoma de México, Ciudad Universitaria, C. P. 04510, México D. F., México; and Department of Chemistry and Center for Nanoscale Science and Technology, Rice University, MS 222, 6100 Main Street, Houston, Texas 77005

Received: April 22, 1999; In Final Form: July 13, 1999

Ab initio and density functional theory calculations were performed on small Pd clusters to assess their precise energy level characteristics. The ground states of Pd and Pd<sub>3</sub> are found to be singlets while Pd<sub>2</sub> and Pd<sub>4</sub> are triplets. Pd<sub>2</sub> is found to be a weak dimer with bond energy of 18 kcal/mol. The trimer is triangular and the tetramer is of tetrahedral geometry. A nonadditive effect can be observed as the size of cluster increases. Larger clusters are bonded better than smaller ones. The second lowest state of Pd<sub>4</sub> is a singlet of tetrahedral geometry. Modern DFT methods yield results of better quality than sophisticated standard ab initio methods, thereby providing an affordable avenue for the analysis of larger clusters and potential nanoelectronics probes.

## 1. Introduction

Recent developments in modern density functional theory (DFT)<sup>1–6</sup> have permitted the extension of calculations to transition metal moieties with precisions that were previously only possible for molecules containing first- and second-row atoms. Modern functionals like the generalized gradient approximation (GGA) and their combination into hybrid functionals permit one to obtain accuracies in energetics better than several of the existing standard ab initio methods.<sup>5,7–9</sup> Previous results with these functionals have been very promising, despite the fact that the hybrid functionals have been designed using information from experimental values of molecules containing only first- and second-row atoms. Even with these recent developments, clusters of transition metals remain a challenge for state-of-the-art computational techniques. In particular, the study of small Pd clusters is of fundamental importance in several areas of basic and applied chemistry.<sup>10</sup> Research on catalysis motivates ongoing efforts to improve existing technologies or to invent new technologies, making this field of widespread strategic importance.<sup>11</sup> Additionally, and central to our interests, the design and fabrication of nanostructured electronic devices is founded upon experiments of conductivity on single molecules attached to nanoscale metal electrodes which are going to influence the measurements within the metal–molecule–metal junction.<sup>12–17</sup> Thus, a precise understanding of the nanoclusters is required previous to the evaluation of the electronic behavior in molecular systems. Given the nanoscale nature of the tips used to connect single molecules, small clusters provide a perfect representation of a real tip, much better than using surfaces or bulk representations. Nanotips and their connection to other chemical moieties like “alligator clips” are of major importance for the precise determination and analysis of single-molecule electronic devices, which may become an integral part of future nanoprocessors.<sup>18–20</sup>

## 2. Theory and Methods

Modern DFT is based on the Hohenberg–Kohn theorems,<sup>21</sup> the Kohn–Sham procedure,<sup>22</sup> and the Levy amend.<sup>23</sup> It has

become a suitable tool for precise ab initio computational chemistry. Starting from the nonrelativistic time independent electronic Schrödinger equation

$$\hat{H}\Psi = E\Psi \quad (1)$$

of a system with Hamiltonian

$$\hat{H} = \hat{T} + \sum \hat{v}_{\text{ext}} + \hat{V}_{\text{ee}} \quad (2)$$

the energy of the electronic system is given exactly by

$$E = T_s + \int d\vec{r} v_{\text{ext}}(\vec{r})\rho(\vec{r}) + \int_0^1 d\lambda \langle \Psi_\lambda | \hat{V}_{\text{ee}} | \Psi_\lambda \rangle \quad (3)$$

In this expression,  $\Psi_\lambda$  always yields  $\rho$ , the electron density of the real system (i.e., when  $\lambda = 1$ )<sup>24</sup> and it is the exact solution of

$$\hat{H}_\lambda \Psi = E_\lambda \Psi_\lambda \quad (4)$$

where

$$\hat{H}_\lambda = \hat{T} + \sum v_\lambda + \lambda \hat{V}_{\text{ee}} \quad (5)$$

The parameter  $\lambda$ ,<sup>25</sup> known as the adiabatic connection parameter sets the external potential  $v_\lambda$  to constraint an invariant  $\rho$  for any  $\lambda \in [0, 1]$ .<sup>24</sup>

The integral in  $\lambda$  has not been expressed in terms of an exact computable expression, but very good approximations have been reported when it is partitioned following the Kohn–Sham procedure<sup>26</sup>

$$\int_0^1 d\lambda \langle \Psi_\lambda | \hat{V}_{\text{ee}} | \Psi_\lambda \rangle = \frac{1}{2} \int d\vec{r} d\vec{r}' \frac{\rho(\vec{r})\rho(\vec{r}')}{|\vec{r} - \vec{r}'|} + E_{\text{xc}}[\rho] \quad (6)$$

where

$$\frac{1}{2} \int d\vec{r} d\vec{r}' \frac{\rho(\vec{r})\rho(\vec{r}')}{|\vec{r} - \vec{r}'|} = V_{\text{class}} \quad (7)$$

from where the  $E_{\text{xc}}[\rho]$ , the exchange–correlation energy, is unambiguously defined. This partitioning allowed a straight-

<sup>†</sup> University of South Carolina.

<sup>‡</sup> Universidad Nacional Autónoma de México.

<sup>§</sup> Rice University.

**TABLE 1: Huzinaga and Huzinaga-E (Extended) Basis Sets for the Pd Atom<sup>a</sup>**

type	$\zeta_i$		
	Huzinaga(17s11p8d)	Huzinaga-E(17s11p8d3f)	
S	722049.07	722049.07	
	109352.6	109352.6	
	25013.151	25013.151	
	7155.5559	7155.5559	
	2398.15	2398.15	
	905.94369	905.94369	
	374.64803	374.64803	
	165.14908	165.14908	
	64.119284	64.119284	
	28.719757	28.719757	
	10.579348	10.579348	
	5.4118888	5.4118888	
	2.2499606	2.2499606	
	1.1164752	1.1164752	
	0.48448268	0.48448268	
	0.11247078	0.11247078	
	0.040067417	0.040067417	
	P	5841.5992	5841.5992
		1369.8311	1369.8311
		439.60614	439.60614
167.49952		167.49952	
71.086943		71.086943	
32.278302		32.278302	
14.685368		14.685368	
6.8062951		6.8062951	
3.0304099		3.0304099	
1.3134192		1.3134192	
0.50827979		0.50827979	
D	242.47077	242.47077	
	71.709317	71.709317	
	27.050913	27.050913	
	11.168119	11.168119	
	4.7897946	4.7897946	
	1.9901245	1.9901245	
	0.77945515	0.77945515	
F	0.26602317	0.26602317	
		1.00	
		0.20	
		0.04	

<sup>a</sup> A Gaussian basis set is defined as a contraction of Gaussian functions where  $N$  is the number of contractions.  $\chi = \sum_{i=1}^N c_i x^k y^l z^m e^{-\zeta_i r^2}$ . If  $N = 1$  we have an uncontracted Gaussian.  $c_i = 1.0$  implies an uncontracted basis set. Grouped functions with  $c_i \neq 1.0$  imply a basis made of contracted Gaussians (s-type function, when  $k + l + m = 0$ ; p-type function when  $k + l + m = 1$ ; and d-type function when  $k + l + m = 2$ , etc.).

forward simplification for the uniform electron gas (jellium) model that further permit us to obtain exact local functionals. These local functionals are used as a starting point in present and more complex functionals like the generalized gradient approximation (GGA), and the hybrid or fully nonlocal functionals. Once the exchange-correlation functional is approximated, the following equation can be solved in a self-consistent field (SCF) manner<sup>27</sup>

$$\left[ -\frac{1}{2}\nabla^2 + \hat{v}_{\text{ext}} + \hat{v}_{\text{class}} + \hat{v}_{\text{xc}} \right] \varphi_i = \epsilon_i \varphi_i \quad (8)$$

until convergence is achieved, yielding the Kohn–Sham orbitals and one-electron energies of a system of noninteracting electrons. The total energy of the system is obtained as well as the wave function of a noninteracting system whose density is identical to the real one.

Within this framework of theory, the analysis of the Pd compounds was performed using the DFT methods as provided by the program Gaussian-94.<sup>28</sup> We have used two basis sets

**TABLE 2: LANL2DZ and LANL-E (Extended) Basis Sets for the Pd Atom<sup>a</sup>**

type	LANL2DZ (8s6p4d//3s3p2d)		LANL-E (13s7p5d1f//8s4p3d1f)	
	$\zeta_i$	$c_i$	$\zeta_i$	$c_i$
S	2.787	-1.610239	2.787	-1.610239
	1.965	1.848984	1.965	1.848984
	0.6243	0.6037492	0.6243	0.6037492
	2.787	1.354078	2.787	1.354078
	1.965	-1.678085	1.965	-1.678085
	0.6243	-0.8559381	0.6243	-0.8559381
	0.1496	1.02003	0.1496	1.02003
	0.0436	1.0	0.0436	1.0
			0.019	1.0
			0.01	1.0
P	5.999	-0.103491	5.999	-0.103491
	1.443	0.7456952	1.443	0.7456952
	0.5264	0.3656494	0.5264	0.3656494
	0.7368	0.0763285	0.7368	0.0763285
	0.0899	0.9740065	0.0899	0.9740065
	0.0262	1.0	0.0262	1.0
D	6.091	0.0376146	6.091	0.0376146
	1.719	0.5200479	1.719	0.5200479
	0.6056	0.5706071	0.6056	0.5706071
	0.1883	1.0	0.1883	1.0
F			0.09	1.0
			0.8	1.0

<sup>a</sup> See footnote in Table 1 for explanation.

for the full-electron Pd clusters calculations: the double- $\zeta$  valence plus polarization,<sup>29</sup> which is a (18s, 12p, 9d) contracted to (6s, 5p, 3d), and the uncontracted Huzinaga's (17s, 11p, 8d).<sup>30</sup> We have also increased the size of the largest basis set. The extended basis sets were made based on our earlier experience with the Au atoms.<sup>14</sup> The Huzinaga basis set was increased by adding three f-functions with exponents 1.00, 0.20, and 0.04 as shown in Table 1. We have also used effective core potentials to represent the core electrons in the Pd atom. This seems to be a powerful tool to incorporate relativistic effects in the calculations and it is a good compromise with the alternative use of full-electron procedures since it reduces the required computational effort without loss of accuracy.<sup>31</sup> The basis set used for the Pd atom is the Los Alamos National Laboratory (LANL) set for effective core potentials (ECP) of double- $\zeta$  type (LANL2DZ).<sup>32–34</sup> We have also increased the standard ECP LANL2DZ with five s, one p, one d, and one f functions thereby obtaining the LANL-E basis set which is shown in Table 2 together with the original LANL2DZ. We have used the hybrid functionals B3LYP and B3PW91 as well as the GGA's PW86, BP86, and BPW91. They combine the Becke exchange (B) functional,<sup>35</sup> the Lee–Yang–Parr (LYP) correlation functional,<sup>36</sup> the Perdew–Wang–86 exchange functional,<sup>37</sup> the

**TABLE 3: Pd Atomic Energies ( $E_h$ ) of the Ground and the First Excited Triplet States, Singlet–Triplet Separation Energy (kcal/mol), and Errors with Respect to the Experimental Separation Energy (kcal/mol) Using Several Levels of Theory**

method/basis set <sup>a</sup>	singlet	triplet	separation	error
HF/Huzinaga-E	-4937.791 20	-4937.789 12	1.3	-20.3
HF/LANL-E	-125.867 25	-125.865 25	1.3	-20.3
HF/LANL2DZ	-125.864 84	-125.862 11	1.7	-19.9
HF/LANL-E <sup>c</sup>	-125.867 25	-125.862 39	3.0	-18.6
HF/Huzinaga	-4937.791 20	-4937.785 84	3.4	-18.2
MP2/LANL2DZ	-125.979 52	-125.969 23	6.5	-15.1
HF/DZVP	-4937.250 35	-4937.229 49	13.1	-8.5
MP3/LANL2DZ	-125.954 49	-125.931 17	14.6	-7.0
CISD/LANL2DZ	-125.957 88	-125.934 11	14.9	-6.7
CCSD/LANL2DZ	-125.961 07	-125.935 66	15.9	-5.7
MP3/Huzinaga	-4937.900 90	-4937.875 39	16.0	-5.6
CISD/Huzinaga	-4937.901 69	-4937.875 93 <sup>b</sup>	16.2	-5.4
CISD/LANL-E	-126.121 88	-126.095 89	16.3	-5.3
MP3/LANL-E <sup>c</sup>	-125.963 30	-125.937 18	16.4	-5.2
MP3/LANL-E	-126.129 51	-126.103 08	16.6	-5.0
QCISD/LANL2DZ	-125.963 78	-125.937 32	16.6	-5.0
CCSD/Huzinaga	-4937.905 70	-4937.878 38 <sup>b</sup>	17.1	-4.5
BD(T)/LANL2DZ	-125.967 04	-125.939 53	17.3	-4.3
CCSD(T)/LANL2DZ	-125.967 48	-125.939 89	17.3	-4.3
QCISD/Huzinaga	-4937.906 14	-4937.878 63	17.3	-4.3
QCISD(T)/LANL2DZ	-125.968 52	-125.940 59	17.5	-4.1
CCSD(T)/Huzinaga	-4937.908 04	-4937.879 87 <sup>b</sup>	17.7	-3.9
QCISD(T)/Huzinaga	-4937.908 24	-4937.879 98	17.7	-3.9
CCSD/LANL-E	-126.135 59	-126.107 34	17.7	-3.9
CCSD/LANL-E <sup>c</sup>	-125.971 47	-125.942 24	18.3	-3.3
MP4SDTQ/Huzinaga	-4937.909 62	-4937.880 17	18.5	-3.1
QCISD/LANL-E	-126.139 62	-126.109 45	18.9	-2.7
CCSD(T)/LANL-E	-126.144 40	-126.113 67	19.3	-2.3
QCISD(T)/LANL-E	-126.145 50	-126.114 40	19.5	-2.1
B3LYP/LANL2DZ	-126.706 76	-126.675 27	19.8	-1.8
B3LYP/Huzinaga	-4940.173 99	-4940.141 97	20.1	-1.5
PW86/Huzinaga <sup>c</sup>	-4940.673 75	-4940.641 30	20.4	-1.2
MP2/Huzinaga	-4937.911 74	-4937.879 05	20.5	-1.1
B3PW91/LANL2DZ	-126.748 71	-126.715 56	20.8	-0.8
MP4SDTQ/LANL2DZ	-125.975 31	-125.941 82	21.0	-0.6
B3LYP/LANL-E <sup>c</sup>	-126.712 50	-126.678 98	21.0	-0.6
PW91/Huzinaga <sup>c</sup>	-4940.660 42	-4940.626 11	21.5	-0.1
B3PW91/LANL-E	-126.753 01	-126.718 58	21.6	0.0
experimental <sup>d</sup>			21.6	
B3LYP/LANL-E	-126.712 50	-126.677 89	21.7	0.1
B3P86/LANL2DZ	-127.119 83	-127.084 49	22.2	0.6
B3PW91/Huzinaga-E	-4940.227 15	-4940.191 01	22.7	1.1
B3PW91/Huzinaga	-4940.227 15	-4940.190 71	22.9	1.3
BP86/LANL2DZ	-126.758 90	-126.720 99	23.8	2.2
MP3/DZVP	-4937.297 37	-4937.259 22	23.9	2.3
BP86/Huzinaga	-4940.605 33	-4940.566 70	24.2	2.6
MP4SDTQ/LANL-E	-126.156 00	-126.116 94	24.5	2.9
CCSD/DZVP	-4937.302 38	-4937.262 74 <sup>b</sup>	24.9	3.3
BPW91/Huzinaga	-4940.463 06	-4940.423 23	25.0	3.4
B3P86/Huzinaga	-4941.328 03	-4941.288 26	25.0	3.4
CISD/DZVP	-4937.302 58	-4937.262 55 <sup>b</sup>	25.1	3.5
MP4SDTQ/LANL-E <sup>c</sup>	-125.988 16	-125.948 18	25.1	3.5
MP2/LANL-E <sup>c</sup>	-125.979 52	-125.939 34	25.2	3.6
MP3/Huzinaga-E	-4938.059 69	-4938.018 11	26.1	4.5
MP2/LANL-E	-126.155 97	-126.114 27	26.2	4.6
CCSD/Huzinaga-E	-4038.061 10	-4938.019 36	26.2	4.6
QCISD/DZVP	-4937.305 73	-4937.263 39	26.6	5.0
CCSD(T)/Huzinaga-E	-4038.067 10	-4038.023 38	27.4	5.8
CCSD(T)/DZVP	-4937.310 05	-4937.265 07	28.2	6.6
MP4SDTQ/Huzinaga-E	-4938.068 76	-4038.023 53	28.4	6.8
MP2/DZVP	-4937.301 98	-4937.256 00	28.9	7.3
QCISD(T)/DZVP	-4937.311 63	-4937.265 44	29.0	7.4
MP2/Huzinaga-E	-4938.079 83	-4938.026 64	33.4	11.8
MP4SDTQ/DZVP	-4937.317 48	-4937.264 14	33.5	11.9
PW86/DZVP	-4939.880 22	-4939.824 79	34.8	13.2
B3LYP/DZVP	-4939.688 36	-4939.632 75	34.9	13.3
B3PW91/DZVP	-4939.735 10	-4939.678 73 <sup>b</sup>	35.4	13.8
B3P86/DZVP	-4940.834 45	-4940.777 05	36.0	14.4
BLYP/DZVP	-4939.705 00	-4939.645 01	37.6	16.0
BP86/DZVP	-4940.122 39	-4940.061 22	38.4	16.8
BPW91/DZVP	-4939.983 80	-4939.922 01	38.8	17.2

<sup>a</sup> Basis sets LANL-E and Huzinaga-E are extensions of the LANL2DZ and Huzinaga basis sets, respectively. <sup>b</sup> Convergence at  $10^{-6}$ . <sup>c</sup> Reference 9. <sup>d</sup> Reference 52. <sup>e</sup> No f-functions were used but other s, p, and d were added.

Perdew–86 correlation functional,<sup>38</sup> and the Perdew–Wang–91 correlation functional,<sup>39</sup> which are nonlocal generalized gradient approximated functionals.<sup>39–41</sup> In addition, the B3 indicates a three fitted parameter functional where a portion of the exchange contribution has been calculated in the same fashion as in the Hartree–Fock (HF) procedure,<sup>42</sup> but using the KS noninteracting wave function instead of the HF wave function. In addition to comparisons to the scarce experimental values available for Pd clusters, we have also performed standard ab initio calculations using the HF, MP2, MP3, MP4SDTQ, CISD, QCISD, BD(T), and CCSD methods. In both cases, DFT and standard ab initio methods, we use full-electron and effective core potential calculations.

### 3. Results and Discussion

Table 3 shows the total energies for the singlet and triplet lowest states of atomic Pd using several levels of theory. Since the singlet–triplet separation is well-known experimentally, 21.6 kcal/mol, this should be a good starting point to determine the level of theory to be used for other systems. Table 3 shows that the B3PW91/LANL-E has a perfect match with the experimental value. Also excellent results are obtained with the PW91/HUZINAGA and the B3LYP/LANL-E levels of theory, which have errors of only 0.1 kcal/mol. Other levels of theory are within chemical accuracy. The DFT methods PW91/HUZINAGA, B3LYP/LANL-E, B3PW91/LANL-E, B3P86/LANL2DZ, and B3PW91/LANL2DZ yield errors smaller than 1 kcal/mol; the ab initio MP4SDTQ/LANL2DZ is within this category. Table 3 also shows a systematic improvement of the standard ab initio methods when improving the level of theory. However, it was practically impossible to obtain convergence with the larger basis sets for full electron calculations. Most of the ab initio methods underestimate the single–triplet separation energy, for example, as expected they tend to stabilize the triplets. Errors of around 5–10 kcal/mol are common when working with transition metals. We can also observe in Table 3 that except for the isolated case of PW91/HUZINAGA, only procedures with relativistic corrections yield chemical accuracy. However, nonrelativistic procedures yield errors smaller than 2–3 kcal/mol. Apparently, this is the range of energy of the relativistic effects in the singlet–triplet separation energy of the Pd atom. We also notice that extending the Huzinaga basis set does not result in an improvement of the singlet–triplet separation of the Pd atom; however, extending the basis set of the procedures with relativistic corrections provides results that are encouragingly good. Results for the singlet–triplet separation energy are not good when the small basis DZVP is used with DFT or ab initio methods. With the other basis sets, DFT results are always of good quality and standard ab initio methods like HF, MP, CC, or QCI cannot yet compete. Ignoring the DZVP basis sets, the DFT errors are at most 3.4 kcal/mol while the standard correlated ab initio methods can result in errors ~10 kcal/mol. The best ab initio results are obtained with MP4SDTQ/LANL2DZ, followed by MP2/HUZINAGA, QCISD(T)/LANL-E, CCSD(T)/LANL-E, MP3/DZVP, and MP4SDTQ/LANL-E. The convergence criteria for the SCF were set to  $10^{-8}$  for all calculations. Very few cases of poor SCF convergence are indicated in Table 3, attained only by the nonrelativistic methods. The convergence with the relativistic corrected methods was usually smooth. The electronic structure of the ground state of Pd atom is  $1s^2 2s^2 2p^6 3s^2 3p^6 3d^{10} 4s^2 4p^6 4d^{10} 1S_0$  and the triplet corresponds to a  $1s^2 2s^2 2p^6 3s^2 3p^6 3d^{10} 4s^2 4p^6 4d^9 5s^1 3D_1$  ( $J = 3, 2, 1$ ) corresponding to experimental levels of 6564.11, 7754.99, and 10 093.94  $\text{cm}^{-1}$ , respectively, with

**TABLE 4: Pd Neutral and Positive Ion Energies ( $E_h$ ), Ionization Potential IP (kcal/mol), and Error (kcal/mol) with Respect to the Experimental IP**

method/basis set	Pd	Pd <sup>+</sup>	IP	error
HF/Huzinaga-E	-4937.791 20	-4937.576 51	134.7	-57.6
MP3/Huzinaga-E	-4938.059 69	-4937.790 93	168.6	-22.6
CCSD/Huzinaga-E	-4938.061 10	-4937.790 67	169.7	-22.6
CCSD(T)/Huzinaga-E	-4938.067 10	-4937.794 23	171.2	-21.1
MP4SDTQ/Huzinaga-E	-4938.068 76	-4937.794 41	172.2	-20.1
MP3/Huzinaga-E	-4938.079 83	-4937.796 62	177.7	-14.6
HF/LANL2DZ	-125.864 84	-125.629 10	147.9	-44.3
B3LYP/Huzinaga	-4940.173 99	-4939.935 28	149.8	-42.4
HF/Huzinaga-E <sup>b</sup>	-4937.823 06	-4937.579 35	152.9	-39.3
MP3/LANL2DZ	-125.954 49	-125.685 41	168.9	-23.3
CISD/LANL2DZ	-125.957 88	-125.687 55	169.6	-22.5
CCSD/LANL2DZ	-125.961 07	-125.688 40	171.1	-21.1
QCISD/LANL2DZ	-125.963 78	-125.689 55	172.1	-20.1
CCSD(T)/LANL2DZ	-125.967 48	-125.691 54	173.2	-19.0
QCISD(T)/LANL2DZ	-125.968 52	-125.692 00	173.5	-18.7
MP3/Huzinaga-E <sup>b</sup>	-4937.942 40	-4937.664 93	174.1	-18.1
CISD/LANL-E	-126.121 88	-125.841 80	175.8	-16.4
MP2/LANL2DZ	-125.969 23	-125.687 72	176.7	-15.5
MP4SDTQ/LANL2DZ	-125.975 31	-125.693 09	177.1	-15.1
MP3/LANL-E	-126.129 50	-125.847 33	177.1	-15.1
CCSD/LANL-E	-126.135 59	-125.849 89	179.3	-12.9
QCISD/LANL-E	-126.139 62	-125.851 38	180.9	-11.3
CCSD(T)/LANL-E	-126.144 40	-125.854 60	181.9	-10.3
QCISD(T)/LANL-E	-126.145 50	-125.855 06	182.3	-9.9
B3PW91/Huzinaga-E <sup>b</sup>	-4940.227 15	-4939.936 27	182.5	-9.7
MP4SDTQ/Huzinaga-E <sup>b</sup>	-4937.961 77	-4937.669 99	183.1	-9.1
MP2/Huzinaga-E <sup>b</sup>	-4937.959 70	-4937.667 82	183.2	-9.0
MP4SDTQ/LANL-E	-126.156 00	-125.857 05	187.6	-4.6
MP2/LANL-E	-126.155 97	-125.854 45	189.2	-3.0
experimental <sup>a</sup>			192.3	
B3PW91/LANL2DZ	-126.748 71	-126.434 36	197.3	5.1
B3LYP/LANL2DZ	-126.706 76	-126.390 99	198.2	6.0
B3PW91/LANL-E	-126.753 01	-126.436 23	198.8	6.6
B3LYP/LANL-E	-126.712 50	-126.392 29	200.9	8.7

<sup>a</sup> References 53 and 54. <sup>b</sup> No f-functions used but additional s, p, and d functions added.

respect to the ground state. The  $J$ -average from these three values yields the experimental singlet–triplet separation energy of 21.6 kcal/mol.

HF yields better results using full-electron calculations. This might result because the relativistic errors tend to cancel those from correlation. HF always overestimates the singlet–triplet energy, indicating that it always favors the triplet. The largest error is obtained with the largest basis set, indicating a total imbalance between correlation and relativistic cancellations. Our calculations permit us to observe that the inclusion of f-functions in the basis sets is of about 2 kcal/mol when using ECP and about 15 kcal/mol when using full-electron calculations. At the MP2 level, the errors are systematically reduced favoring the singlet state. The largest error is still obtained with the largest basis set but favoring the singlet and not the triplet as yielded with the HF method. The errors using ECP with the extended basis sets are acceptable and an excellent result is obtained with the Huzinaga basis set (1.1 kcal/mol of error). However, the full-electron calculation yield poor values when using the largest basis sets. In this case, the effect of the f-functions in the basis sets is limited to 1 kcal/mol for the ECP methods and to 5 kcal/mol for the full-electron methods. A systematic reduction of errors can be observed at the MP3 level: none of chemical precision, but all of them smaller than 8 kcal/mol which is an acceptable tolerance for transition metal systems. The effect of the f-functions is reduced to only 0.2 kcal/mol for the ECP methods and to 2 kcal/mol for the full core methods. At the MP4, more precisely MP4SDTQ, the errors



**TABLE 5: Pd Neutral and Negative Ion Energies ( $E_h$ ), Electron Affinity EA (kcal/mol), and Error (kcal/mol) with Respect to the Experimental EA Energy**

method/basis set	Pd	Pd <sup>-</sup>	EA	error
B3LYP/LANL-E	-126.712 50	-126.392 29	-200.9	-213.8
B3PW91/LANL-E	-126.753 01	-126.436 23	-198.8	-211.6
CCSD/LANL-E	-126.135 59	-125.849 89	-179.3	-192.1
CISD/LANL-E	-126.121 88	-125.841 80	-175.7	-188.6
HF/LANL2DZ	-125.864 84	-125.813 58	-32.2	-45.0
HF/Huzinaga-E	-4937.791 20	-4937.745 37	-28.8	-41.6
MP3/Huzinaga-E	-4938.059 69	-4938.019 84	-25.0	-37.8
CCSD/Huzinaga-E	-4938.061 10	-4938.022 49	-24.2	-37.0
CCSD(T)/Huzinaga-E	-4938.067 10	-4938.028 67	-24.1	-36.9
MP4SDTQ/Huzinaga-E	-4938.068 76	-4938.030 46	-24.0	-36.8
MP2/Huzinaga-E	-4938.079 83	-4938.041 96	-23.8	-36.6
MP3/LANL2DZ	-125.954 49	-125.918 75	-22.4	-35.3
MP2/LANL2DZ	-125.969 23	-125.934 76	-21.6	-34.5
CISD/LANL2DZ	-125.957 88	-125.923 69	-21.5	-34.3
CCSD/LANL2DZ	-125.961 07	-125.928 97	-20.1	-33.0
QCISD/LANL2DZ	-125.963 78	-125.932 82	-19.4	-32.3
MP4SDTQ/LANL2DZ	-125.975 31	-125.945 91	-18.5	-31.3
CCSD(T)/LANL2DZ	-125.967 48	-125.938 12	-18.4	-31.3
QCISD(T)/LANL2DZ	-125.968 52	-125.940 06	-17.9	-30.7
B3PW91/Huzinaga-E	-4940.227 15	-4940.208 73	-11.6	-24.4
HF/Huzinaga-E <sup>b</sup>	-4937.823 06	-4937.821 67	-0.9	-13.7
HF/LANL-E	-125.867 25	-125.866 02	-0.8	-13.6
MP2/Huzinaga-E <sup>b</sup>	-4937.959 70	-4937.958 78	-0.6	-13.4
MP3/Huzinaga-E <sup>b</sup>	-4937.942 40	-4937.941 46	-0.6	-13.4
B3PW91/LANL2DZ	-126.748 71	-126.748 10	-0.4	-13.2
MP4SDTQ/Huzinaga-E <sup>b</sup>	-4937.961 77	-4937.961 14	-0.4	-13.2
MP3/LANL-E	-126.129 50	-126.129 24	-0.2	-13.0
MP2/LANL-E	-126.155 97	-126.155 93	0.0	-12.9
MP4SDTQ/LANL-E	-126.156 00	-126.156 48	0.3	-12.5
B3LYP/LANL2DZ	-126.706 76	-126.707 48	0.4	-12.4
QCISD/LANL-E	-126.139 62	-126.145 12	3.4	-9.4
CCSD(T)/LANL-E	-126.144 40	-126.155 82	7.2	-5.7
QCISD(T)/LANL-E	-126.145 50	-126.159 39	8.7	-4.1
B3PW91/Huzinaga-E <sup>b</sup>	-4940.265 82	-4940.283 48	11.1	-1.8
experimental <sup>a</sup>			12.8	
B3LYP/Huzinaga-E	-4940.217 80	-4940.238 77	13.2	0.3

<sup>a</sup> Reference 54 and 55. <sup>b</sup> No f-functions but additional s, p, and d functions added.

disperse more than in the MP3, from -3.1 kcal/mol to 14.3 kcal/mol. The largest errors are found using the extended basis set without f-functions for the full core method and the smallest basis set for the ECP method. Excellent results are obtained with the ECP methods, even with the smallest basis set. The effect of the f-functions in the basis sets is of 0.6 kcal/mol for the ECP methods and of 7.5 kcal/mol for the full-electron methods. CCSD(T) and CCSD yield excellent results, namely all with absolute errors of 2–7 kcal/mol. The errors are about 1 kcal/mol better with the CCSD(T) than with the CCSD. The same can be said about the CISD methods; however, errors are ~1–2 kcal/mol larger than with the two CC methods used. The same trend applies to the two QCI methods used in this work, specifically the QCISD and the QCISD(T).

The DFT methods yield the best results for the singlet–triplet separation of the Pd atom. B3LYP yield chemical accuracy (around 1 kcal/mol errors) if not used with the small DZVP basis set, and using f-functions for full-electron calculations. The B3P86 yields similar results. The B3PW91 yields the best results of all the methods used in this work. A perfect match with the experiment is obtained with this functional and with the largest basis set using ECP. Chemical precision is obtained with any other combination of basis sets except that f-functions are needed for full core calculations and basis sets larger than the DZVP for ECP calculations. These two later restrictions hold for all DFT methods used in this work. The effect of the f-function is 0.5 kcal/mol for the ECP methods and 14.8 kcal/mol for the full electron methods. It is also clear from Table 3 that those DFT methods which do not use hybrid functionals

yield excellent results without the use of f-functions. This applies to the BPW86, BPW91, and PW91PW91 functionals, thereby indicating that the need of f-functions may come from the hybrid nature of the B3 exchange functionals.

Table 4 shows the ionization potential (IP) for the Pd atom. We have used only a subset of the methods used to calculate the singlet–triplet separation. Calculations of ionization potentials are usually more difficult than those of the singlet–triplet energies since the former require the calculation of radicals. The smallest error corresponds to the ab initio method MP2/LANL-E, which underestimates the IP by 3 kcal/mol; this is followed by the underestimation given by the more sophisticated MP4SDTQ/LANL-E of 4.6 kcal/mol. Next is the B3PW91/LANL2DZ level of theory with an overestimation of the IP of 5.1 kcal/mol; this latter result represents an error of only 2.7%. This is followed by the B3LYP/LANL2DZ with an error of 6.0 kcal/mol. The QCISD(T)/LANL-E yields an error of 9.9 kcal/mol and the CCSD(T)/LANL-E yields an error of 10.3 kcal/mol. As it was found for the singlet–triplet separation energy, only the ECP, relativistic corrected, yields the best results. We can notice here that the best DFT results overestimate the IP and this overestimation is about 5–6 kcal/mol using the nonrelativistic methods. On the other hand, the standard ab initio methods underestimate the IP, and we can observe a more systematic improvement of the results as the level of theory increases. In this case the convergence of the radicals was too difficult with the larger basis sets. Specifically, truncation errors may have to be considered for energies in the range of 5000  $E_h$  since more than nine decimal figures are needed in order to

**TABLE 6: Total Energies, Bond Lengths, and Dissociation Energies of the Ground State Singlet and the First Excited Triplet State of Pd Dimer Using Several Levels of Theory**

method/basis set	singlet			triplet		
	total energy ( $E_h$ )	$R_e$ (Å)	$D_e$ (kcal/mol)	total energy ( $E_h$ )	$R_e$ (Å)	$D_e$ (kcal/mol)
experimental <sup>a</sup>						16.9, 26.0
B3LYP/DZVP	-9879.388 80	2.897	7.6	<i>b</i>		
B3LYP/Huzinaga	-9880.365 19	2.824	10.8	-9880.366 65	2.559	11.7
B3LYP/LANL2DZ	-253.436 17	2.762	14.2	-253.448 79	2.526	22.1
B3LYP/LANL-E <sup>c</sup>	-253.442 77	2.791	11.2	-253.452 48	2.536	17.3
B3LYP/LANL-E	-253.443 17	2.791	11.4	-253.454 28	2.536	18.4
B3LYP/Huzinaga-E <sup>c</sup>	-9880.445 59	2.872	6.3	-9880.429 98	2.555	-3.5
B3P86/Huzinaga	-9882.672 16	2.789	10.1	-9882.667 10	2.530	6.9
B3PW91/Huzinaga	-9880.469 02	2.810	9.2	-9880.465 17	2.542	6.8
B3PW91/LANL2DZ	-253.519 13	2.745	13.6	-253.531 08	2.504	21.1
B3PW91/LANL-E <sup>c</sup>	-253.524 19	2.770	11.4	-253.534 19	2.513	17.7
B3PW91/LANL-E	-253.524 66	2.770	11.7	-253.536 22	2.513	19.0
B3PW91/Huzinaga-E <sup>c</sup>	-9880.541 27	2.850	6.0	-9880.525 10	2.533	-4.1
HF/LANL2DZ	-251.732 50	3.260	1.8	-251.734 62	2.743	3.1
HF/LANL-E <sup>c</sup>	-251.736 23	3.312	1.1	-251.735 79	2.733	0.8
HF/LANL-E	-251.736 27	3.312	1.1	-251.741 58	2.733	4.4
HF/Huzinaga	-9875.585 17	3.169	1.7	-9875.573 02	2.780	-5.9
HF/Huzinaga-E <sup>c</sup>	-9875.646 33	3.693	0.1	-9875.609 08	2.688	-23.2
MP2/Huzinaga	-9875.828 92	3.006	3.4	-9875.812 66	2.460	-6.8
MP2/LANL2DZ	-251.950 71	2.941	-5.2	-251.932 17	2.458	-16.9
MP2/LANL-E <sup>c</sup>	-251.971 53	2.901	7.8	-251.950 65	2.475	-5.3
MP2/LANL-E	-252.330 84	2.901	11.9	-251.734 05	2.475	-362.6
MP3/Huzinaga	-9875.806 25	3.044	2.8	-9875.793 78	2.501	-5.0
MP3/LANL2DZ	-251.918 57	2.993	6.0	-251.917 84	2.560	5.6
MP3/LANL-E <sup>c</sup>	-251.936 74	2.948	6.4	-251.935 68	2.568	5.7
MP3/LANL-E	-252.272 59	2.948	8.5	-252.272 26	2.568	8.3
MP4SDTQ/DZVP//MP2/DZVP	-9874.641 19	3.106	3.9	-9874.607 86	2.491	-17.0
MP4SDTQ/HUZI//MP2/HUZI	-9875.825 09	3.006	3.7	-9875.815 84	2.480	-2.1
MP4SDTQ/LANL2DZ//MP2/LANL2DZ	-251.966 53	3.006	10.0	-251.955 55	2.480	3.1
MP4SDTQ/LANL-E <sup>c</sup> //MP2/LANL-E <sup>c</sup>	-251.992 74	2.901	10.3	-251.976 28	2.475	0.0
MP4SDTQ/LANL-E//MP2/LANL-E	-252.333 88	2.901	13.7	-252.322 41	2.475	6.5
CCSD/LANL-E <sup>c</sup> //MP2/LANL-E <sup>c</sup>	-251.956 85	2.901	8.7	-251.961 25	2.475	11.5

<sup>a</sup> Reference 43. <sup>b</sup> No convergence. <sup>c</sup> No f-functions were added to the LANL-E and Huzinaga-E, but additional s, p, and d were added.

**TABLE 7: Total Energies, Structural Parameters, and Binding Energy for the Lowest Singlet and Triplet Electronic States of Pd Trimers**

method/basis set	energy ( $E_h$ )	$R_e$ (Å)	$D_e$ (kcal/mol)
singlet			
B3LYP/DZVP ( $D_{3h}$ )	-14819.076 08	2.549	6.9
B3LYP/DZVP ( $D_{\infty h}$ )	-14819.087 63	2.909	14.1
B3LYP/Huzinaga ( $D_{3h}$ )	-14820.589 80	2.545	42.5
B3LYP/Huzinaga ( $D_{\infty h}$ )	-14820.555 03	2.833	20.7
B3PW91/LANL2DZ ( $D_{3h}$ )	-380.330 08	2.496	52.7
B3PW91/LANL-E <sup>a</sup> ( $D_{3h}$ )	-380.306 49	2.810	29.8
B3PW91/LANL-E ( $D_{3h}$ )	-380.307 72	2.810	30.6
B3PW91/LANL2DZ ( $D_{\infty h}$ )	-380.286 20	2.774	25.2
HF/LANL-E <sup>a</sup> ( $D_{3h}$ )	-377.606 26	3.344	2.8
HF/LANL-E ( $D_{3h}$ )	-377.606 37	3.344	2.9
MP2/LANL-E <sup>a</sup> ( $D_{3h}$ )	-377.974 10	2.902	22.3
MP2/LANL-E ( $D_{3h}$ )	-378.522 25	2.902	34.1
MP4/LANL-E <sup>a</sup> //MP2/LANL-E <sup>a</sup> ( $D_{3h}$ )	-377.936 63	2.902	-17.5
MP4/LANL-E//MP2/LANL-E ( $D_{3h}$ )		2.902	
triplet			
B3LYP/DZVP ( $D_{3h}$ )	-14819.103 90	2.697	24.3
B3LYP/DZVP ( $D_{\infty h}$ )	-14819.083 89	2.644	11.8
B3LYP/Huzinaga ( $D_{3h}$ )	-14820.594 91	2.607	45.7
B3LYP/Huzinaga ( $D_{\infty h}$ )	-14820.567 77	2.590	28.7
B3PW91/LANL2DZ ( $D_{\infty h}$ )	-380.283 70	2.616	23.6

<sup>a</sup> No f-functions were used but other s, p, and d were added.

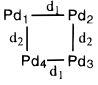
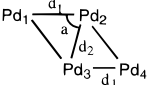
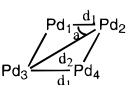


obtain relatively acceptable energy differences. The HF method provides very poor estimations of the IP, about 40 kcal/mol or more. MP2 corrects these errors notably well. With the LANL-E basis set the error is of only of 3 kcal/mol. For an experimental energy of 192.3 kcal/mol this error correspond to only 1.6% of the IP. MP2 with the nonextended basis sets yields much larger errors. IP energies are not improved with the MP3 method. The errors increase with any of the basis sets, indicating that the

convergence of the perturbation series is not trivial for this kind of systems. Errors for the MP3 are about 15 kcal/mol or more using either ECP or full-electron calculations. Energies are improved again at the MP4 level but yielding the same quality of the MP2, which is indicative of the oscillatory behavior of the series. The need of larger basis sets is more notorious here. The inclusion of f-function improves the IP by ~10 kcal/mol. The difference between relativistic and nonrelativistic results

**TABLE 8: (a) Total Energy  $E$  ( $E_h$ ) and Atomization Energies  $\Sigma D_e$  (kcal/mol) for the Lowest Singlet and Triplet Electronic States of Several Pd Tetramers and (b) Optimized Geometries of the Lowest States and Conformations of Pd<sub>4</sub> (Distances in Å, and Angles in deg)**

(a) Total and Atomization Energies				
method/basis set	singlet		triplet	
	$E$	$\Sigma D_e$	$E$	$\Sigma D_e$
B3LYP/DZVP linear	-19758.78730	21.2	-19758.78529	20.0
B3LYP/DZVP square	-19758.80112	29.9	-19758.81121	36.3
B3LYP/DZVP rhombic	no convergence		-19758.82114	42.5
B3LYP/DZVP tetrahedral	-19758.81792	40.5	-19758.84671	58.5
B3LYP/Huzinaga linear	-19760.74515	30.9	no convergence	
B3LYP/Huzinaga tetrahedral	-19760.81981	77.7	-19760.8492*	96.2
B3PW86/DZVP linear	-19763.37764		-19763.37716	
B3PW86/DZVP tetrahedral	-19763.41444		-19763.44975	
B3PW86/Huzinaga tetrahedral	-19765.43692	78.3	-19765.46153	93.8
B3PW91/LANL2DZ linear	-507.05347	36.8	-507.04428	31.0
B3PW91/LANL2DZ $D_{4h}$ square	-507.14160	92.1	-507.14071	91.5
B3PW91/LANL2DZ rhombic $C_{2h}$	-507.13892	90.4	-507.13275	86.5
B3PW91/LANL2DZ trans	-507.14177	92.2	-507.11629	76.2
B3PW91/LANL2DZ tetrahedral	-507.15666	101.6	-507.18315	118.2

(b) Optimized Geometries			
structure	method and point group	singlet	triplet
$\text{Pd}_1 \xrightarrow{d_1} \text{Pd}_2 \xrightarrow{d_2} \text{Pd}_3 \xrightarrow{d_1} \text{Pd}_4$	B3LYP/DZVP $D_{\infty h}$	$d_1 = 2.907$ $d_2 = 2.920$	$d_1 = 2.761$ $d_2 = 2.613$
	B3LYP/Huzinaga $D_{\infty h}$	$d_1 = 2.834$ $d_2 = 2.889$	
	B3PW86/DZVP $D_{\infty h}$	$d_1 = 2.849$ $d_2 = 2.859$	$d_1 = 2.703$ $d_2 = 2.572$
	B3PW91/LANL2DZ $D_{\infty h}$	$d_1 = 2.774$ $d_2 = 2.800$	$d_1 = 2.718$ $d_2 = 2.646$
	B3LYP/DZVP $D_{4h}$ and $D_{2h}$	$d_1 = 2.871$ $d_2 = 2.871$	$d_1 = 2.579$ $d_2 = 2.582$
	B3PW91/LANL2DZ $D_{4h}$	$d_1 = 2.493$ $d_2 = 2.493$	$d_1 = 2.509$ $d_2 = 2.509$
	B3LYP/DZVP $C_{2h}$		$d_1 = 2.771$ $d_2 = 2.658$ $a = 61.4$
	B3PW91/LANL2DZ $C_{2h}$	$d_1 = 2.596$ $d_2 = 2.463$ $a = 61.7$	$d_1 = 2.663$ $d_2 = 2.521$ $a = 60.5$
	B3PW91/LANL2DZ $C_{2h}$	$d_1 = 2.492$ $d_2 = 3.525$ $a = 45.0$	$d_1 = 2.693$ $d_2 = 2.597$ $a = 60.9$
	B3LYP/DZVP $T_d$	$d = 1.653$	$d = 2.449$
	B3LYP/Huzinaga $T_d$	$d = 1.647$	$d = 2.705$
	B3PW86/DZVP $C_{3v}$	$d_1 = 2.780$ $d_2 = 2.658$ $a = 65.0$ $w_{1342} = 60.0$	$d_1 = 2.646$ $d_2 = 2.804$ $a = 57.9$ $w_{1342} = 71.2$
	B3PW86/Huzinaga $C_{2v}$	$d_1 = 2.917$ $d_2 = 2.558$ $a = 55.3$ $w_{1234} = 61.4$	$d_1 = 2.641$ $d_2 = 2.821$ $a = 57.4$ $w_{1234} = 71.7$
	B3PW91/LANL2DZ $C_2$	$d_1 = 2.805$ $d_2 = 2.557$ $d_3 = 2.555$ $d_4 = 2.557$ $a = 66.5$ $w_{2413} = 64.5$	$d_1 = 2.615$ $d_2 = 2.613$ $d_3 = 2.584$ $d_4 = 2.758$ $a = 63.8$ $w_{1234} = 74.7$

is about 5 kcal/mol with the relativistic values being closer to the experiment. CCSD and CCSD(T) methods yield errors similar to those of the MP3 method and the QCISD and QCISD(T) errors approach those of the MP4 methods.

Among the DFT functionals, again the B3PW91 yields acceptable results with errors of 5–10 kcal/mol. Similar errors are obtained with the B3LYP. Again, the need of large basis sets with these two functionals is important. However, the

LANL2DZ basis set yields good results with these two functionals.

A relatively similar situation happens with the electron affinities shown in Table 5. While the B3PW91 and B3LYP functionals with the HUZINAGA-E basis set yield excellent results with errors of only 1.8 and 0.3 kcal/mol, respectively, most of the other expected precise methods yield relative large errors. Even worse, several standard ab initio and DFT methods yield negative electron affinities. We can conclude, with the calculations shown so far, that for the Pd atom the B3PW91 and B3LYP functionals yield acceptable results when the extended basis sets are used. The prediction of the electron affinity (EA) of Pd is difficult due to its small value, 12.8 kcal/mol, which is within the range of tolerance of most of the present methods. All HF calculations predict the anion to be higher in energy than the neutral. Similar results are obtained with MP2 calculations where the best values are shown using the ECP. MP3 and MP4 yield also higher anion energy compared to the neutral Pd, except for MP4/LANL-E, which indicates that the anion is lower in energy than the neutral. These trends in the perturbation series seem to indicate that Pd has a negative EA (i.e., the external electron will leave the atom). Other standard ab initio methods lead us to the same conclusion except when the extended LANL-E basis set is used. Thus, for this exigent situation, the use of relativistic ECP and an extended basis set including f-functions is important to have a good prediction of the EA. A similar situation holds with the DFT methods. The use of relativistic ECP and the use of extended basis sets are important for the prediction of the EA of the Pd atom. The B3PW91 performs much better than the B3LYP for the EA energy.

Table 6 shows the results for the singlet and triplet dimer of Pd. Unfortunately, there are two very different values for the experimental dissociation energy of the assumed ground state.<sup>43</sup> Likewise, there are several sophisticated calculations with a broad range of results,<sup>44,45</sup> although this has been an established Pd<sub>2</sub> singlet ground state. For instance, a combined experimental and HF-CI calculation yielded a singlet as ground state with a dissociation energy of 24 kcal/mol.<sup>46</sup> A smaller value for the bond energy was proposed but still with the singlet as ground state by Blomberg et al.<sup>47</sup> Cui et al. reported identical values to ours for B3LYP/LANL2DZ which are also similar to their reported CASPT2 values.<sup>7</sup> They conclude that the triplet is the ground state for Pd<sub>2</sub>. On the basis of the results in Table 6 and the performance of several levels of theory for Pd calculations, we can confirm that the ground state of the Pd dimer corresponds to a triplet with a bond length of approximately 2.5 Å and a bond energy of about 18 kcal/mol. This is very close to one of the reported experimental energies of 16.9 kcal/mol<sup>43</sup> (also reported in that reference is the other less reliable result of 26.0 kcal/mol). The B3PW91 and B3LYP DFT methods, using relativistic corrections, predict the triplet as the ground state while most standard ab initio methods predict the singlet as the ground state; this is probably why the singlet was assigned as the ground state. On the basis of our atomic calculations and the fact that the experimental binding energy is practically reproduced by the triplet dimers, we are persuaded to conclude that the ground state of Pd<sub>2</sub> corresponds to a triplet configuration. In support of this, we notice that the bond lengths for the triplets are always smaller than the bond length for the singlets. The best predictions with the standard ab initio methods are for the singlet with dissociation energies of ~10 kcal/mol. This same energy is predicted by the DFT methods, however, above the triplet state. The CC method yields the best prediction

among the standard ab initio methods. It also predicts the triplet as ground state with bond energy of 11.5 kcal/mol. Smaller basis sets seem to work better for the dimer than for the monomer as it is expected by the mutual superposition of basis sets. All bond and atomization energies have been calculated by subtracting the energy of the molecule from the sum of energies of the ground-state atoms. MRCIS-INDO calculations also predicted the triplet as the ground state with a bond length of 2.46 and the singlet 10 kcal/mol above the ground.<sup>48</sup> Fahmi and Santen<sup>49</sup> also find the triplet of Pd<sub>2</sub> to be the ground state, however, with a bond energy of 29 kcal/mol. They also found the singlet to be only 4 kcal/mol above the ground state.

For the trimer or larger clusters, only DFT methods are practical and of acceptable precision. The lowest singlet configuration (ground state) corresponds to  $D_{3h}$  symmetry using the relativistic corrections and nonrelativistic methods. For the triplet, the lowest state also corresponds to a  $D_{3h}$  configuration. Notice that the  $D_{3h}$  point group is very important for the treatment of (111) surfaces and the simulations of Pd nanotips. Results for the trimer are shown in Table 7. We can see that the trimer ground state affords greater binding energy per atom than the dimer ground-state per atom. Linear clusters are important in the study of the cluster-bulk evolution.<sup>50</sup> The linear trimer is about 25 kcal/mol above the triangular ground state, and the linear singlet has about the same energy as the linear triplet cluster. The large difference between the linear and triangular triplets may be a problem for the study of one-dimensional clusters, which does not happen with, for instance, Cu clusters.<sup>50</sup>

Table 8a,b shows the optimized geometries of the lowest states of Pd<sub>4</sub>. In all cases, the tetrahedral structure corresponds to the most stable conformer. This is also true for the three multiplicities studied in this work. The ground state for Pd<sub>4</sub> corresponds to the triplet state which is 16.7 kcal/mol below the singlet. For all conformers, the triplet ends up having the lowest energy. The search was oriented to find the ground state of Pd<sub>4</sub> and, therefore, no further emphasis was devoted to study excited states except for the lowest singlet, triplet, and quintet multiplicities.

#### 4. Conclusion

Based on this study, the ground states of the Pd monomer is a singlet, the dimer is a triplet, the trimer is a singlet, and tetramer is a triplet. This is justified by the fact that an even number of atoms does not allow the occupation of the 5s levels, which, of course, is impossible for the monomer and trimer. This effect of stabilization between triangular atomic s-orbitals in the atoms is very similar to the one on the triangular H<sub>3</sub><sup>+</sup> molecule. The geometries of the tetramers show distances that are analogous to expected distances for Pd clusters. For all conformers, the Pd-Pd distance varies between 2.5 and 2.8 Å, which is near the experimental value of 2.75 Å for the Pd-Pd nearest-neighbor length in a Pd metal.

We can conclude that the bond energy for the dimer can be predicted as 18.1 kcal/mol, which is in good agreement with one of the experimental values, 16.9 kcal/mol.<sup>43</sup> The binding energy can be estimated at 30.6 kcal/mol for the trimer and 118.2 kcal/mol for the tetramer. The above values correspond to binding energies per atom of 9.0, 10.2, and 29.6 kcal/mol for the dimer, trimer and tetramer, respectively, indicating a strong nonadditive effect. As expected from small clusters, the energy per atom is far from the experimental cohesive energy, which for Pd crystal is 90.4 kcal/mol.<sup>51</sup>

In summary, we have been able to predict, with reasonably accuracy, the available experimental information on Pd clusters



and predict with confidence the energetics and structures of those clusters that have not yet been characterized. We have found that the B3PW91 and B3LYP functionals used with extended basis sets and relativistic ECP provide excellent results for Pd clusters. The relative energies of all systems are reported with similar accuracy to that obtained with molecules containing first- and second-row atoms. For these small clusters, we confirm that the binding energy per atom increases with the number of atoms in the clusters.

**Acknowledgment.** We highly appreciate the support of DARPA/ONR under grant N00014-99-1-0406, ARO under grant DAAD19-99-1-0085, and the supercomputer support of NASA and M. Frisch from Lorentzian Inc. M. C. deeply acknowledge financial support from DGAPA UNAM under Project IN104798.

## References and Notes

- Parr, R. G.; Yang, W. *Density-functional theory of atoms and molecules*; Clarendon Press: Oxford, England, 1989.
- Kryachko, E. S.; Ludeña, E. V. *Energy density functional theory of many-electron systems*; Kluwer Academic: Dordrecht, 1990.
- Gross, E. K. U.; Dreizler, R. M.; North Atlantic Treaty Organization. Scientific Affairs Division. *Density functional theory*; Plenum Press: New York, 1995.
- Seminario, J. M.; Politzer, P., Eds. *Modern Density Functional Theory: A Tool for Chemistry*; Elsevier: Amsterdam, 1995; p 405.
- Seminario, J. M., Ed. *Recent Developments and Applications of Modern Density Functional Theory*; Elsevier: Amsterdam, 1996; p 900.
- Seminario, J. M., Ed. *Advances in Quantum Chemistry: Density Functional Theory*; Academic Press: New York, 1998.
- Cui, Q.; Musaev, D. G.; Morokuma, K. *J. Chem. Phys.* **1998**, *108*, 8418–8428.
- Seminario, J. M.; Tour, J. M. *Int. J. Quantum Chem.* **1997**, *65*, 749–758.
- Seminario, J. M.; Zacarias, A. G.; Castro, M. *Int. J. Quantum Chem.* **1997**, *61*, 515–523.
- Somarjai, G. A. *Introduction to Surface Chemistry and Catalysis*; Wiley: New York, 1994.
- Lambert, R. M.; Pacchioni, G., Eds. *Chemisorption and Reactivity of Supported Clusters and Thin Films Towards an Understanding of Microscopic Processes in Catalysis*; Kluwer: Dordrecht, 1997.
- Purcell, S. T.; Garcia, N.; Binh, V. T.; Jones II, L.; Tour, J. M. *J. Am. Chem. Soc.* **1994**, *116*, 11985.
- Seminario, J. M.; Tour, J. M. In *Molecular Electronics: Science and Technology*; Aviram, A.; Ratner, M., Eds.; Annals of the New York Academy of Sciences: New York, 1998; pp 68–94.
- Seminario, J. M.; Zacarias, A. G.; Tour, J. M. *J. Am. Chem. Soc.* **1999**, *121*, 411–416.
- Seminario, J. M.; Tour, J. M. In *Proceedings of the International Workshop on Electron Correlations and Materials Properties*; Gonis, A., Ed.; in press.
- Seminario, J. M.; Zacarias, A. G.; Tour, J. M. *J. Phys. Chem. A*, in press.
- Seminario, J. M.; Zacarias, A. G.; Tour, J. M. *J. Am. Chem. Soc.* **1998**, *120*, 3970–3974.
- Wu, R.; Schumm, J. S.; Pearson, D. L.; Tour, J. M. *J. Org. Chem.* **1997**, *61*, 6906–6921.
- Bumm, L. A.; Arnold, J. J.; Cygan, M. T.; Dunbar, T. D.; Burgin, T. P.; Jones, L. II.; Allara, D. L.; Tour, J. M.; Weiss, P. S. *Science* **1996**, *271*, 1705–1707.
- Tour, J. M.; Kosaki, M.; Seminario, J. M. *J. Am. Chem. Soc.* **1998**, *120*, 8486–8493.
- Hohenberg, P.; Kohn, W. *Phys. Rev. B* **1964**, *136*, 864–871.
- Kohn, W.; Sham, L. J. *Phys. Rev. A* **1965**, *140*, 1133–1138.
- Levy, M. *Proc. Natl. Acad. Sci. U.S.A.* **1979**, *76*, 6062–6065.
- Langreth, D. C.; Perdew, J. P. *Solid State Commun.* **1975**, *17*, 1425–1429.
- Harris, J.; Jones, R. O. *J. Phys. F* **1974**, *4*, 1170–1186.
- Seminario, J. M. In *Modern Density Functional Theory: A Tool for Chemistry*; Seminario, J. M., Politzer, P., Eds.; Elsevier: Amsterdam, 1995; pp 1–27.
- Parr, R. G.; Yang, W. *Density Functional Theory of Atoms and Molecules*; Oxford University Press: Oxford, UK, 1989.
- Frisch, M. J.; Trucks, G. W.; Schlegel, H. B.; Gill, P. M. W.; Johnson, B. G.; Robb, M. A.; Cheeseman, J. R.; Keith, T.; Petersson, G. A.; Montgomery, J. A.; Raghavachari, K.; Al-Laham, M. A.; Zakrzewski, V. G.; Ortiz, J. V.; Foresman, J. B.; Ciolowski, J.; Stefanov, B. B.; Nenayakkara, A.; Challacombe, M.; Peng, C. Y.; Ayala, P. Y.; Chen, W.; Wong, M. W.; Andres, J. L.; Replogle, E. S.; Gomperts, R.; Martin, R. L.; Fox, D. J.; Binkley, J. S.; Defrees, D. J.; Baker, J.; Stewart, J. P.; Head-Gordon, M.; Gonzalez, C.; Pople, J. A. *Gaussian 94*; E.I version; Gaussian, Inc.: Pittsburgh, PA, 1996.
- Godbout, N.; Salahub, D. R. *Can. J. Chem.* **1992**, *70*, 560.
- Huzinaga, S. *J. Chem. Phys.* **1977**, *66*, 4245.
- Neyman, K. M.; Pacchioni, G.; Rösch, N. In *Recent Developments and Applications of Modern Density Functional Theory*; Seminario, J. M., Ed.; Elsevier: Amsterdam, 1996; pp 569–619.
- Hay, P. J.; Wadt, W. R. *J. Chem. Phys.* **1985**, *82*, 270–283.
- Hay, P. J.; Wadt, W. R. *J. Chem. Phys.* **1985**, *82*, 299–310.
- Wadt, W. R.; Hay, P. J. *J. Chem. Phys.* **1985**, *82*, 284–298.
- Becke, A. D. *Phys. Rev. A* **1988**, *33*, 3098.
- Lee, C.; Yang, W.; Parr, R. G. *Phys. Rev. B* **1988**, *37*, 785–789.
- Perdew, J. P.; Wang, Y. *Phys. Rev. B* **1986**, *33*, 8800–8802.
- Perdew, J. P. *Phys. Rev. B* **1986**, *33*, 8822–8824.
- Perdew, J. P. In *Electronic Structure of Solids*; Ziesche, P., Eschrig, H., Eds.; Akademie Verlag: Berlin, 1991; pp 11–20.
- Perdew, J. P.; Chevary, J. A.; Vosko, S. H.; Jackson, K. A.; Pederson, M. R.; Singh, D. J.; Fiolhais, C. *Phys. Rev. B* **1992**, *46*, 6671–6687.
- Perdew, J. P.; Wang, Y. *Phys. Rev. B* **1992**, *45*, 13244–13249.
- Becke, A. D. *J. Chem. Phys.* **1993**, *98*, 5648–5652.
- Lin, S. S.; Strauss, B.; Kant, A. *J. Chem. Phys.* **1969**, *51*, 2282–2283.
- Balasubramanian, K. *J. Chem. Phys.* **1988**, *89*, 6310.
- Goursot, A.; Papai, I.; Salahub, D. R. *J. Am. Chem. Soc.* **1992**, *114*, 7452.
- Shim, I.; Gingerich, K. A. *J. Chem. Phys.* **1984**, *80*, 5107–5119.
- Blomberg, M. R. A.; Lebrilla, C. B.; Siegbahn, P. E. M. *Chem. Phys. Lett.* **1988**, *150*, 522–528.
- Estiu, G. L.; Zerner, M. C. *J. Phys. Chem.* **1994**, *98*, 4793–4799.
- Fahmi, A.; van Santen, R. A. *J. Phys. Chem.* **1996**, *100*, 5676–5680.
- Balbuena, P. B.; Derosa, P. A.; Seminario, J. M. *J. Phys. Chem. B* **1999**, *103*, 2830–2840.
- Lide, D. R., Ed. *CRC Handbook of Chemistry and Physics*; CRC Press: Boca Raton, FL, 1998.
- Moore, C. E. *Table of Atomic Energy Levels*; U.S. National Bureau of Standards: Washington, DC, 1971.
- Lias, S. G. *J. Phys. Chem. Ref. Data* **1988**, *17*.
- Lide, D. R. *Handbook of Chemistry and Physics*, 74th ed.; CRC Press: Boca Raton, FL, 1994.
- Hotop, H.; Lineberger, W. C. *J. Phys. Chem. Ref. Data* **1985**, *14*, 731.